Pressure Dependent Elastic, Mechanical and Ultrasonic Properties of ZnO Nanotube

Aadesh K Prajapati[a], Sachin Rai[a], Kuldeep[b,c] & Pramod K Yadawa[a*]

[a]Department of Physics, Prof. Rajendra Singh (Rajju Bhaiya) Institute of Physical Sciences for Study and Research,
V. B. S. Purvanchal University, Jaunpur 222 003, India
[b]CSIR-National Physical Laboratory, Dr. K. S. Krishnan Marg, New Delhi-110 012, India
[c]Academy of Scientific and Innovative Research (AcSIR), Ghaziabad, Uttar Pradesh, 201 002, India

ZnO Nanotube with an hcp structure, has been investigated for the transmission of acoustic wave in the 0 to 10 GPA operating pressure. For this, the Lennard-Jones interaction potential methodology has been utilizing to estimate the advanced order elastic coefficients (SOECs and TOECs). This model is used to calculate the 2nd and 3rd order elastic parameters for ZnO Nanotube. Applying SOECs, the additional elastic moduli for ZnO nanotubes, for example the bulk modulus (B), Young's modulus (Y), as well as shear modulus (G), have been computed. Later, applying SOECs as well as zincoxide density under the same pressure range, three orientation dependent acoustic velocities, comprising Debye average velocities, have been studied. Basic thermal characteristics such as specific heat at constant volume (C_V), thermal conductivity k $_{(min)}$ associated with lattice, thermal energy density (E_0), thermal relaxation time (τ) as well as acoustic coupling coefficients (D_L, D_S) of ZnO Nanotube have been also calculated at same pressure range. Determining the acoustic attenuation parameters using the method is also successful, arises due to the interaction of phonons, hardness as well as melting temperature under various pressure in this research work.

Keywords: Ultrasonic properties; Thermo-physical characteristics; Zinc oxide nanotube; Second Order Elastic Constants (SOECs), Third Order Elastic Constants (TOECs)

1 Introduction

Several types of nanostructures have piqued curiosity as Nano-building bricks for a variety of exciting uses over the last twenty years. Many distinct types of nanostructures, including such nanotubes, nanowires, and Nano belts, have the potential to be used as upcoming key components for various Nano devices in electronics, photonics & nanoelectro mechanical devices. Regarding thin-film photovoltaic cells constructed on silicon wafers, ZnO film is often used as n-type conductive windows in particular. Many attempts have been undertaken in recent years to synthesize and apply nanoscale zinc oxide-nanomaterials[1–4]. For instance, we looked into the junction configuration of ZnO tetrapod's, which could help us better understand their growth process and applications[5]. ZnO is a mineral that naturally occurs, and its intense pressure phases may be relevant geological formations as a constituent of the lesser mantle. Zinc oxide nanotube solidifies in different shapes: wurtzite (B4), cubic zinc blende (B3), as well as rare cubic rock salt (B1). Under atmospheric

pressure, the wurtzite arrangement is the furthermost persistent and consequently the most prevalent. The zinc and oxide centers are tetrahedral in both circumstances. Furthermore, the rock - salt pattern is only visible at large pressures of approximately 10 GPA. CVD technique is one of the most straight forward and extensively utilized ways for fabricating Zinc oxide nanotubes. A lot of readings reveal wurtzite structure (B4) happens in nanoscale ZnO materials generated by CVD, but the zinc blend (B3) pattern exists in limited numbers[4,6]. Moreover, further research into the elastic characteristics at a lot of pressure could increase the use of ZnO nanoparticles. Different approaches have been used to produce numerous communal types of quasi-anisotropic, inorganic, 1-Dzinc oxide nanostructures such as nanotubes, nanowires, Nano sheets, Nano shells, and Nano helices[7]. 1-D Nano rods have gained a lot of attention in recent decades as they have amazing properties that are dissimilar from those seen in bulk zinc oxide nanomaterials, owing to its high surface-to-volume proportion, distinctive geometrical, as well as quantum size effects. These 1-D NRs are thought to be valuable basic structure block and pose the

greatest contest to a wide range of Nano electronics, resulting in potentially interesting devices such as nanoscale interconnects[8], active ingredients of electro-optic electronic devices[9], field effect transistors[10], Nano cantilevers[11], as well as Nano generators[12]. When nanostructures are utilized in Nano devices, they are often distorted to some amount. Clearly, a detailed and improved comprehension of a nanostructure's mechanical characteristics is required before this Nano material can be effectively included into Nano device construction. Because physical reliability will decide, to some amount, the long-term performance and stability of various Nano devices, it is critical to comprehend the mechanical features of these zinc oxide Nano rods ahead to any useful uses. Not only will this research help in the design and production of the next sensors and actuators, but it will also improve our understanding of nanoscale dynamics, small-scale coupling of electrical and mechanical properties, and multi - physics modelling. The mechanical characteristics of single zinc oxide (ZnO) nanotubes are investigated in this work.

Current study, we only concentrated on the thermo-physical, elastic, as well as mechanical properties of ZnO nanotubes under compression. This nanotube will aid in the research of mechanical performance and play a vital part in the development of manufacturing machinery with convenient mechanical belongings under practical operating circumstances. The effect of pressure on ZnO nanotube is that, it changes lattice parameter. Lattice parameter is directly related to elastic constants, since all elastic, mechanical, and thermo-physical properties that has been describe in this paper depend on elastic constants. So we can see, the effect of pressure on ZnO nanotube. However, a solid's physical properties are crucial because they correlate to a number of essential solid-state characteristics, including inter atomic potentials, equations of state, as well as phonon spectra. Additionally, the specific heat at constant volume, anisotropy constant, thermal attenuation, thermal relaxation time, Poisson's ratio, melting temperature, Young's modulus, Bulk modulus, Debye temperature, Pugh's proportion (B/G), acoustic coupling constants, shear modulus as well as hardness are all thermodynamically related to elastic characteristics.

2 Theoretical Calculation Method

In appearance there are abundant tools for examining hcp compounds' high-order flexible characteristics. Permitting to our current efforts,

higher order elastic constants are being evaluated utilizing interaction-potential techniques.

By using potential model method of evaluation shows that, the higher order coefficients in hexagonally arranged materials are influenced by the crystallite size. The succeeding mathematical formulations can be consumed to govern the SOECs quantities[13].

$$C_{IJ} = \frac{\partial^2 U}{\partial e_I \partial e_J}; \text{I or J} = 1,......6 \qquad ...(1)$$

$$C_{IJK} = \frac{\partial^3 U}{\partial e_I \partial e_J \partial e_K}; I \text{ or } J \text{ or } K = 1,......6 \qquad ...(2)$$

Where $e_I = e_{ij}$ (i or j = x, y, z, I=1…6) stands for a constituent of the tensor of straining as well as U shows elastic energy band. For hcp structural materials, Eqn. 1 as well as Eqn. 2, yields six 2nd order also ten 3rd order elastic constants, correspondingly[14,15].

For acoustic propagation via a z-axis in hcp crystal, the acoustic velocities (V_S and V_L) are provided by equations[15].

$$V_L = \sqrt{\frac{C_{33}}{\rho}} \qquad ...(3)$$

$$V_S = \sqrt{\frac{C_{44}}{\rho}} \qquad ...(4)$$

The density of hcp material scan be evaluated consuming the mathematical formulae given inferior to[16].

$$d = 2Mn/3\sqrt{3}a^2cN_A \qquad ...(5)$$

The letters n, M, as well as N_A, respectively, stand for the quantity of atoms in a single cell, molecular mass, as well as Avogadro number.

Within least-temperature acoustics, the Debye mean velocity (V_D) is an important number since acoustic velocities are connected to elastic coefficients. Debye velocity (V_D) is well-defined as[15].

$$V_D = \left[\frac{1}{3}\left(\frac{1}{V_L^3} + \frac{1}{V_{s1}^3} + \frac{1}{V_{s2}^3}\right)\right]^{-1/3} \qquad ...(6)$$

Elastic factors have an unintentional correlation with Debye temperature (T_D) via Debye velocity.[17]

$$T_D = \hbar V_D (6\pi^2 n_a)^{\frac{1}{3}}/k_B \qquad ...(7)$$

Here k_B, na are the atomic absorption constant and the Boltzmann constant, respectively. Temperature-dependent phonons' energy distribution is hampered by the conveyance of acoustic wave. The length of time required for thermal acoustic waves to re-establish just after acoustic wave has passed through a material is known as that of the thermal repose period (τ). It has a strong relationship to Debye velocity, specific heat, and thermal conductivity[14,18].

$$\tau = \tau_S = \tau_L/2 = \frac{3k}{C_V V_D^2} \qquad \ldots(8)$$

We used the Voigt & Reuss techniques to estimate the bulk elastic factor and the stiffness of shear[19,20]. Unchanging stress and strain computations were employed in the Voigt and Reuss techniques, one-to-one. Additionally, using Hill's approaches, the calculated numeric values that emerge from B and G are computed using the expected values of the sequential procedure[21]. In addition, Hill's techniques are used to subtract the quantitative value that arise from B besides G using the expected values of the balancing procedure[22,23]. We assess the corresponding formulations for G, B, as well as Y:

$$\left.\begin{array}{l} M = C_{11} + C_{12} + 2C_{33} - 4C_{13}, C^2 = (C_{11} + C_{12})C_{33} - 4C_{13} + C^2_{13}; \\ B_R = \frac{C^2}{M}; B_V = \frac{2(C_{11} + C_{12}) + 4C_{13} + C_{33}}{9}; \\ G_V = \frac{M + 12(C_{44} + C_{66})}{30}; G_R = \frac{5C^2 C_{44} C_{66}}{2[3B_V C_{44} C_{66} + C^2(C_{44} + C_{66})]}; \\ Y = \frac{9GB}{G + 3B}; B = \frac{B_V + B_R}{2}; G = \frac{G_V + G_R}{2}; \sigma = \frac{3B-2G}{2(3B + G)} \end{array}\right\} \quad (9)$$

The following mathematical formula can be used to determine a metal's thermal conductivity[24].

$$k = AMT_D^3\delta^3/\gamma^2 T n^{2/3} \qquad \ldots(10)$$

Wherever A is the persistent, γ is Grüneisen number, as well as T stands for temperature. The value, 'A' is calculated by the Grüneisen magnitude as well as is articulated as follows.

$$A = 2.43 \times 10^{-8}/(1 - \frac{0.514}{\gamma} + \frac{0.228}{\gamma^2}) \qquad \ldots(11)$$

The elastic constants C_{11} and C_{33} are interrelated to the Temperatures that melt (Tm) of hcp crystals[25]. The melting point (Tm) is considered in the succeeding technique:

$$T_m = 354 + 4.5(2C_{11} + C_{33})/3 \qquad \ldots(12)$$

Wherever C_{11} as well as C_{33} are in GPA also Tm is in K.

At small temperatures, the average distance travelled by electrons is comparable to the average path of acoustical vibrations. As a consequence, there is a good chance that acoustic phonons as well as free electrons will interact[15,26]. For longitudinal (V_L) as well as shear waves (V_S), the mathematical expressions for evaluating ultrasonic attenuation is given as follows:

$$\alpha_{long} = \frac{2\pi^2 f^2}{\rho V_l^3}\left(\frac{4}{3}\eta_e + \chi\right) \qquad \ldots(13)$$

$$\alpha_{shear} = \frac{2\pi^2 f^2}{\rho V_S^3}\eta_e \qquad \ldots(14)$$

Wherever 'f' is wave's frequency, 'ρ' is the solidity of hcp metal, 'ηe' is the viscosity due to the electron as well as 'χ' is the viscosity due to compression. In order to attenuate acoustic waves at higher pressure, both thermo-elastic loss as well as Akhieser's type loss are crucial. The attenuation resulting from the Akhieser's loss discovered by Rai et al. is described by the mathematical model that is displayed below[27].

$$(\alpha/f^2)_{Akh} = 4\pi\,2\tau E_0\,(D/3)/\,2\rho V^3 \qquad \ldots(15)$$

Thermodynamically generated energy density is denoted by E0, whereas the ultrasound wave's frequency is denoted by f.

The mathematical expression which is given below, considers the thermo-elastic loss (α / f^2) Th:

$$(\alpha/f^2)_{Th} = 4\pi^2 <\gamma_i^j>^2 \frac{kT}{2\rho V_L^5} \qquad \ldots(16)$$

The overall acoustic attenuation is calculated using the equation below:

$$(\alpha/f^2)_{Total} = (\alpha/f^2)_{Th} + (\alpha/f^2)_L + (\alpha/f^2)_S \qquad \ldots(17)$$

Anywhere $(\alpha/f^2)_{Th}$ is the thermo-elastic loss, $(\alpha/f^2)_L$ and $(\alpha/f^2)_S$ are the acoustic wave attenuation quantities for the longitudinal acoustic wave as well as shear acoustic wave consistently.

3 Results and Discussion

3.1 Higher Order Elastic Coefficients and Related Parameters

In this paper, we examined six SOECs & ten TOESs using the fundamental interactions potential approach. For the ZnO nanotube, the lattice factors 'a' (basal plane factor) 'p' (axial proportion) and Density (ρ:x 10^3 kg m^{-3}), are 3.283 (Å) to 3.213 (Å), 1.613 to 1.610 and 5.433 to 5.798 under pressure range
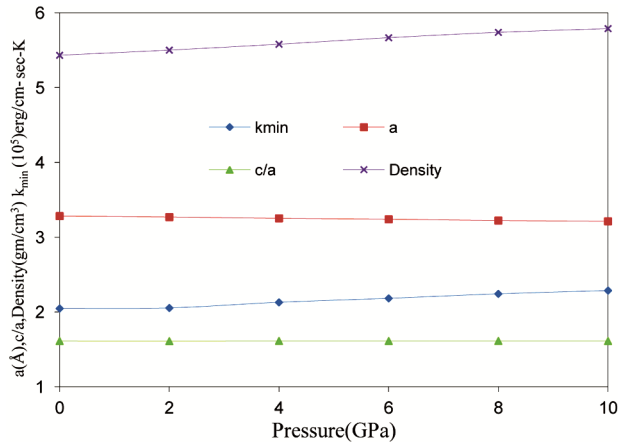
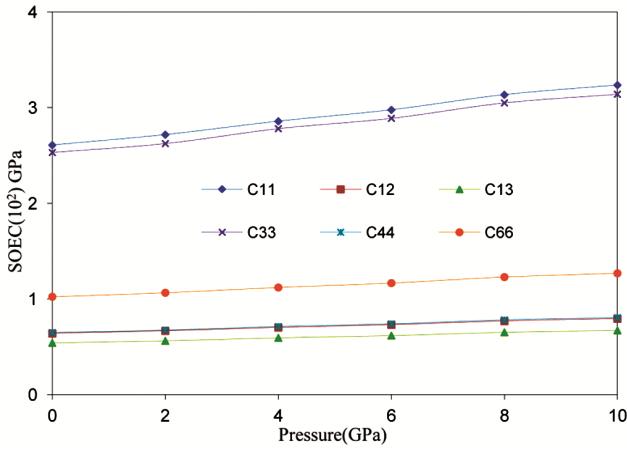Fig. 1 — a (Å), c/a, Density, Thermal conductivity *vs* Pressure of ZnO nanotube.

Fig. 3 — TOECs *vs* Pressure of ZnO nanotube.
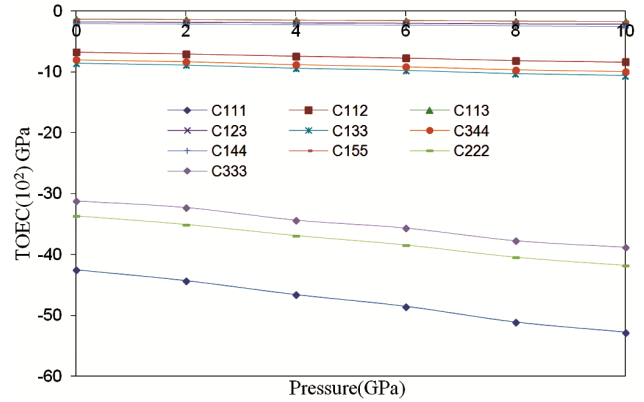

Fig. 2 — SOECs *vs* Pressure of ZnO nanotube.

Fig. 4 — C_{44}- P *vs* Pressure of ZnO nanotube.

Where $\acute{C}_{jj}= \acute{C}_{jj} -P$, (P=1, 3, 5). $\acute{C}_{12}=C_{12}+P$, $\acute{C}_{13}=C_{13}+P$

respectively[26].Computed numeric values of thermal conductivity (k $_{(min)}$ Erg/cm-sec-K) is shown in Fig. 1. For ZnO nanotube, the suggested numeric values of m as well as n stand 6 and 7. For the ZnO nanotube, b_0 value is 2.9×10^{-64} erg cm[7].

The ZnO nanotube contains the elastic parameter estimates, which are important for the composite structure since they relate to the stiffness parameter. In Fig. 2 we can see that second order elastic constants are cumulative by pressure. Fig. 3 shows that the third order elasticity coefficients (TOECs) have a negative numeric value and that their value rises with pressure. The adequate elastic correlation coefficients for zinc oxide nanotubes indicate that they possess superior mechanical properties to other substances.

Born-Huang stability criteria[27,28] satisfied by zinc oxide nanotube and are given below.

$\acute{C}_{44} >0$, $\acute{C}_{11}-| \acute{C}_{12}| > 0$, $(\acute{C}_{11}+ \acute{C}_{12}) \acute{C}_{33} -2 \acute{C}^2_{13}> 0$, …(18)

Due to the fact that the aforementioned elastic measured values are significant, the ZnO nanotube satisfies the criterion for Born-mechanical Huang stability, indicating that its elastic modulus rises within the specified pressure range Fig. 4.

The assessed numeric value of bulk elastic modulus of ZnO nanotube is 124.87 GPA at zero pressure, which is nearly identical as 124.28 GPA calculated Wang *et al.*[26]. The coefficients C_{11}, C_{33}, as well as C_{66} are increased by equivalent amounts using our method. Our theoretical strategy for assessing SOECs of hcp organized metals is therefore well supported. The Voigt and Reuss constants M, C^2 are increases with pressure can be understood in Fig. 5. The numeric values of B, G also Y of ZnO nanotube at pressure range (0 to 10GPA) are slightly increases with pressure, can calculated by consuming Equation 9 besides remaining in Fig. 6. Thus, we can directly see the impact of pressure on different parameters of ZnO nanotube.

The SOECs allow for the evaluation of all mechanical characteristics, including toughness, brittleness, ductility, hardness, as well as compressibility. The melting point being taken into consideration when creating better materials. It is regarded as a crucial foundation for assessing engineering materials. Materials scientists intentionally raise the temperature at which melting occurs in an effort to increase the high thermal resistance of any industrially useful materials. In current work, the hardness and melting point temperature T_m of
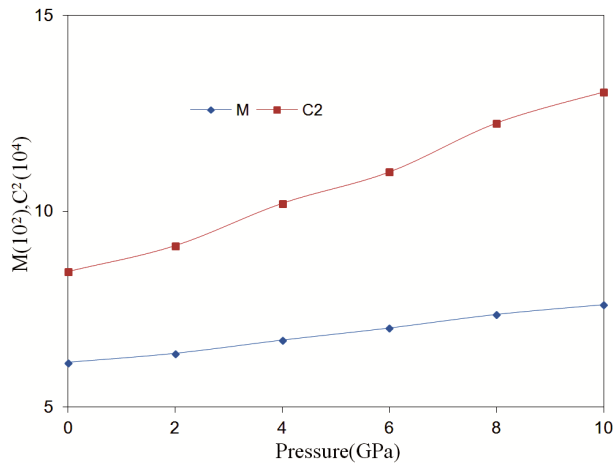
Fig. 5 — M, C^2 *vs* Pressure of ZnO nanotube.
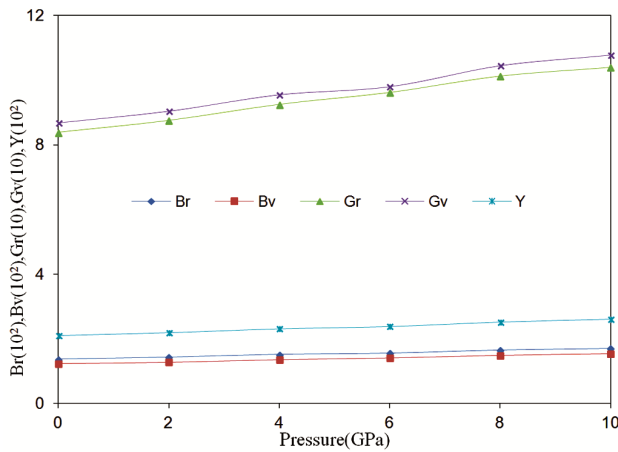
Fig. 6 — B_r, B_v, G_v, G_r, Y *vs* Pressure of ZnO nanotube.

ZnO nanotube is evaluated. Fig. 7 illustrates the approximated melting point temperature as a consequence of the useful pressure. One can observe that as pressure rises, melting temperature rises as well as. It is evident that as pressure rises, melting temperature rises along with it.

As illustrated in the Table 1, anisotropy in elastic properties can be described by the Omni-anisotropic index (A^U), shear elastic anisotropic features (A_1, A_2 as well as A_3), besides percent anisotropy (A_B as well as A_G) is provided below[29,30]. By Table 1, its reveal that under different pressure points for ZnO nanotube, percent anisotropy A_B is higher than A_G. This demonstrates that the orientation of the shear strength differs from the orientation of the bulk elastic modulus. Table 1 delivers that A_1, A_2, and A_3 results under several pressure. The metal is an isotropic crystal if $A_1 = A_2 = A_3 = 1$. Strong single crystalline anisotropy is the term used to describe how far the universal anisotropy value (A^U) deviates from zero at different pressures[31,32].

3.2 Velocity of Ultrasonic Waves and Related Parameters

The isotropic also mechanical characteristics of the compound with a hexagonal lattice were related to ultrasonic velocity in this investigation. In current work, the relationship between ultrasonic velocity and
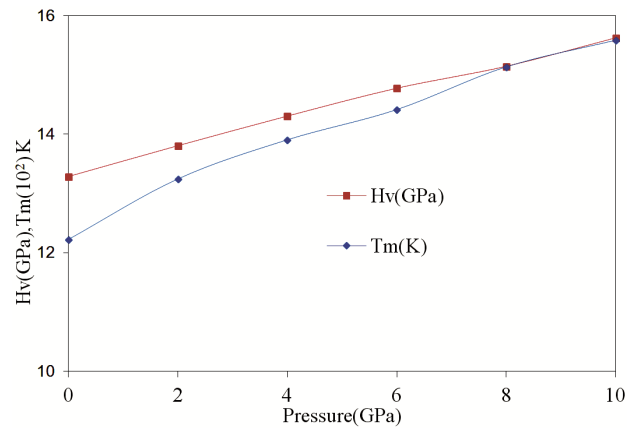
Fig. 7 — Hardness (H_v), Melting temperature (T_m) *vs* Pressure of ZnO nanotube.

Table 1 — Anisotropy coefficients as well as Poisson ratio of ZnO nanotube.							
Pressure (GPa)	A^U	A_B	A_G	A_1	A_2	A_3	σ
0	0.086	0.049	0.017	0.64	0.64	2.08	0.23
2	0.067	0.055	0.016	0.64	0.64	2.07	0.23
4	0.057	0.055	0.016	0.64	0.64	2.08	0.23
6	0.060	0.050	0.015	0.64	0.64	2.08	0.23
8	0.046	0.022	0.014	0.64	0.64	2.06	0.23
10	0.044	0.052	0.014	0.64	0.64	2.08	0.23
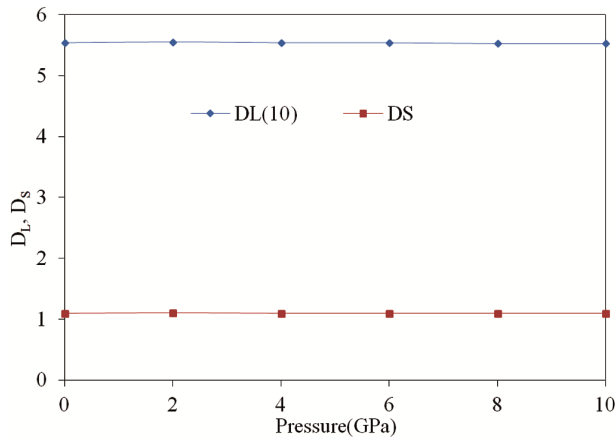
Fig. 8 — D_L, D_S *vs* Pressure of ZnO nanotube.

Fig. 9 — E_0, C_V *vs* Pressure of ZnO nanotube.

Fig. 10 — V_L *vs* "Θ"$_L$ of ZnO nanotube.
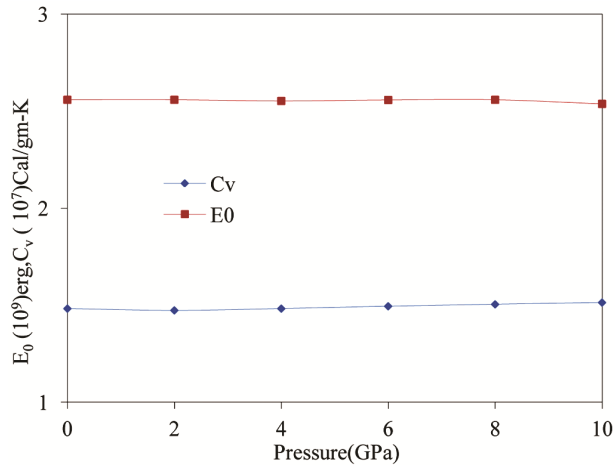

Fig. 11 — V_{S1} *vs* "Θ" of ZnO nanotube.

Fig. 12 — V_{S2} *vs* "Θ" of ZnO nanotube.

the isotropic and mechanical characteristics of the hcp organized materials is examined. Fig. 8 shows the acoustic coupling coefficients (D_L as well as D_S) with pressure. The numeric values of C_V as well as E_0 are calculated consuming the physical coefficients are shown in Fig. 9.

Figures 10-13 depict the relationship between acoustic velocities and pressure. Fig. 10, shows that for ZnO nanotube value of V_L has the least value at 45°, as well as the numeric value of velocity V_{S1} has a supreme value at angle 55° in Fig. 11 & 12 demonstrates that V_{S2} rises with angle and the z-axis. Similar to the confederation velocity curvatures observed in this experiment, alignment velocity curves recorded in other hexagonal substances have been seen[30,31].

Figure 13 illustrates in what way the variation in Debye mean velocity is influenced by the angle through the crystal's unique alliance. For the ZnO nanotube, V_D
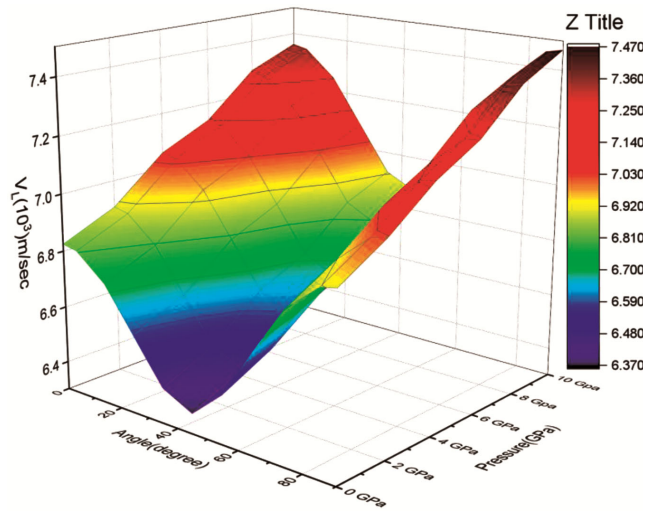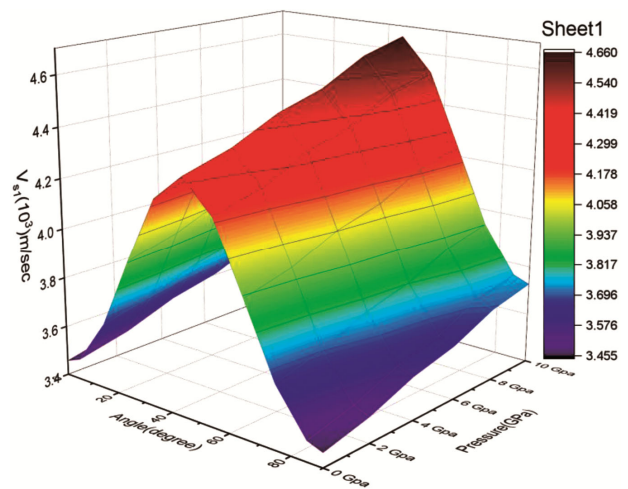
Fig. 13 — V_D *vs* "Θ" of ZnO nanotube.

Fig. 15 — Long & Shear attenuation *vs* Pressure of ZnO nanotube.
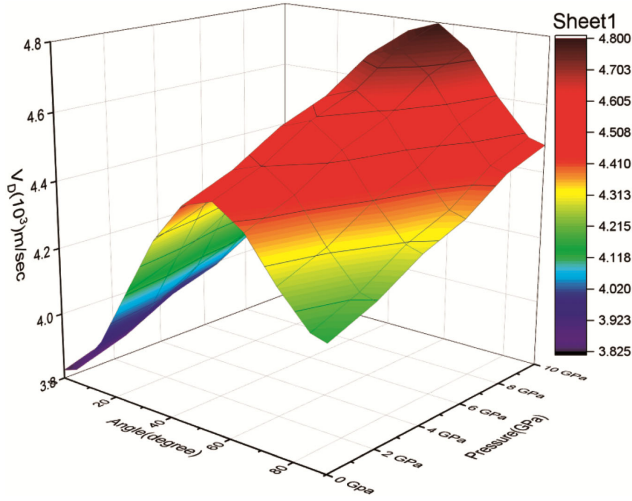

Fig. 14 — Relaxation time *vs* "Θ" with z- axis of crystal of ZnO nanotube.
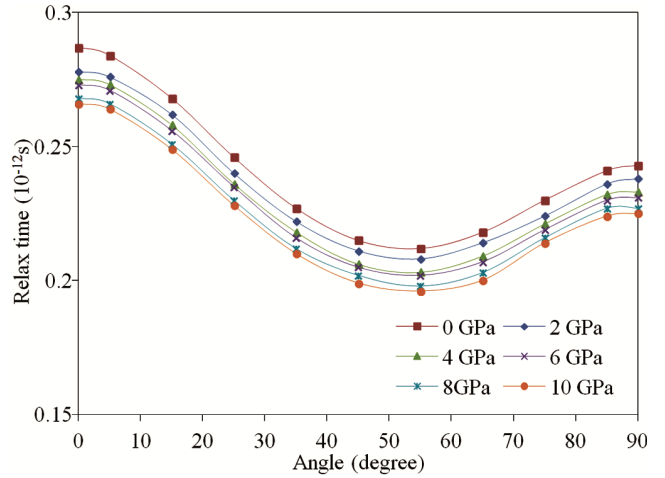
Fig. 16 — Th attenuation *vs* Pressure of ZnO nanotube.

upsurges through angle as well as reaches an extreme at 55°. Due to the fact that the velocities V_{S2}, V_{S1} also V_L are utilized in the calculation of V_D[33,34]. The peak value of V_D is produced at 55° by a significant increase in longitudinal wave velocity as well as shear wave velocity. Additionally, quasi-shear wave velocity is reduced. As soon as an acoustic wave propagate at 55° degree along crystal unique axis, the regular ultrasound wave velocity is maximum.

Figure 14 depicts a diagram of the estimated time required for thermal relaxing as a consequence of angle. The mutual relationship of V_D as $\tau \propto 3k/C_V V_D^2$ is observed by direction reliant curvatures. The period of thermal repose of the ZnO nanotube is undoubtedly subjective by 'k', the duration of thermal relaxation is measured in pico-seconds[33,34]. The value of thermal relaxation time is minimum when the wave
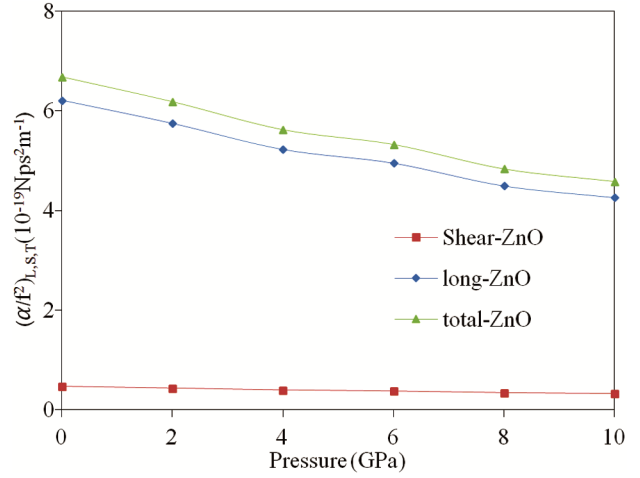
spread along = 55° indicates that the time to re-establish for thermal phonon distribution of equilibrium will be shortest for wave spread in this way due to p-p collaboration as well as relaxation due to heat, attenuation of ultrasonic waves occurs.

3.3 Ultrasonic Wave Attenuation Caused by Phonon-Phonon Interaction and the Thermal Relaxation Mechanism

When estimating the ZnO nanotube's ability to attenuate ultrasonic waves, the wave is anticipated to move along the element's z-axis. The attenuation coefficient divide by the square of the frequency $(\alpha/f^2)_{Akh}$ is deliberate for longitudinal acoustic wave $(\alpha/f^2)_L$ and for shear acoustic wave $(\alpha/f^2)_S$ using Eqns. 13, 14 and 15. Figs. 15 & 16 represent the pressure dependent longitudinal, shear, total and thermo elastic attenuations respectively.

In this current work, it is anticipated that the acoustic wave will move along the z-axis of the crystal. It is understandable that the Akh. Kind of energy waste $(\alpha/f^2)_{Akh}$ be contingent on the D, E_0, τ and V^{-3} (Eqns. 15). E_0 as well as the k significantly affect Akhieser losses in ZnO nanotube.

Because of this, the ability to transfer heat is less effective, which causes an increase in acoustic attenuation. As a conclusion, the phonon-phonon interaction affects ultrasonic attenuation; yet, because there is no conceptual or practical support in the works compiled, a comparison of UA attenuation is not practicable. Eqns. 16 and 17's calculation of total attenuation both demonstrate that the thermo-elastic degradation of ZnO nanotubes is significantly below than Akhieser loss. The main contributing factor is ultrasound attenuation associated to p-p interactions for longitudinal elastic wave as well as shear elastic wave. The main factors affecting overall attenuation are heat energy density as well as thermal conductivity. Given that the ZnO nanotube moves at the fastest speeds at 10Pa, A $\propto$ V³ ought to be greatest at this pressure and the materials ought to be most bendable. The lowest Absorption of Ultrasound Waves (UA) values for ZnO nanotubes preserve their stable hexagonal geometric state under a variety of stresses.

4 Conclusions

In current theoretical approach, the interaction potential technique is used to evaluate the mechanical as well as thermodynamic properties of the ZnO nanotube under pressures oscillating from 0 to 10 GPA. At various pressures, the idea of calculating higher-order elastic coefficients for hcp shaped ZnO nanotube using an easy interaction potential methodology is still relevant. Born-Huang mechanical stability standard demonstrates that, within the operating pressure, for ZnO nanotube mechanical stability increases with pressure. According to the Pugh's proportion, the hexagonal ZnO nanotube is bendable under both normal and the given pressure range, and its ductility rises as pressure rises. Additionally, we discovered that ZnO nanotube exhibits strong anisotropy at zero GPA, which intensifies with increasing pressure. With increasing pressure, the Debye mean velocity rises as well asat that time losses. Pressure raises the estimated melting point and toughness of ZnO nanotube.

The hardness (H_v) rises efficiently by means of increasing pressure up to it beats 0-10 GPA. 'τ' is

revealed in pico-seconds for ZnO nanotube, protecting their hcp form. Since 'τ' has the tiniest value alongside = 55° at altogether pressures and the time important for re-establishing acoustic phonon consistency spreading will be the tiny for acoustical wave transmission in this direction. The primary factor in overall attenuation produced by the p-p strong dealings is thermal conductivity. These findings will serve as the foundation for forthcoming investigation into the thermo-physical properties of additional matters.

Conflict of Interest

There are no competing interests declared by the authors.

References

1   Black K, Chalker P R, Jones A C, King P J, Roberts J L & Heys P N, *Chem Vapor Depos*, 16 (2010) 106.
2   He F Q & Zhao Y P, *J Phys D*, 40 (2007) 1211.
3   Li W J, Shi E W, Zhong W Z & Yin Z W, *J Cryst Growth*, 203 (1999) 186.
4   Okada T, Kawashima K & Ueda M, *Appl Phys A*, 81 (2005) 907.
5   Wang B B, Xie J J, Yuan Q Z & Zhao Y P, *J Phys D*, 41 (2008) 102005.
6   Music S, Saric A & Popovic S, *Ceram Int*, 36 (2010) 1117.
7   Özgür Ü, Alivov YI, Liu C, Teke A, Reshchikov M A, Doğan S, Avrutin V, Cho S J & Morkoç H, *J Appl Phys*, 98 (2005) 041301.
8   Chen C Q, Shi Y, Zhang Y S, Zhu J & Yan Y J, *Phys Rev Lett*, 96 (2006) 075505.
9   He J H, Ho S T, Wu T B, Chen L J & Wang Z L, *Chem Phys Lett*, 435 (2007) 119.
10   Wang X, Zhou J, Song J, Liu J, Xu N & Wang Z L, *Nano Lett*, 6 (2006) 2768.
11   Hughes W L & Wang Z L, *Appl Phys Lett*, 82 (2003) 2886.
12   Wang Z L & Song J, *Science*, 312 (2006) 242.
13   Pandey D K, Yadawa P K & Yadav R R, *Mater Lett*, 61 (2007) 5194.
14   Yadawa P K, *The Arab J Sci Eng*, 37 (2012) 255.

15 Yadav N, Singh S P,Maddheshiya A K,Yadawa P K & Yadav R R, *Phase Trans*, 93 (2020) 883.

16 Pandey D K & Pandey S, *Sciyo Croatia*, 111(2010) 397.

17 Pillai S O, *Solid State Physics*, 7th Edn, (New Age International Publisher, 2005) 100.

18 Singh D, Pandey D K,Yadawa P K & Yadav A K, *Cryogen*, 16 (2009) 12.

19 Yadawa P K, *J Pure Appl Ultrason*, 40 (2018) 16.

20 Yadawa P K, Singh D, Panday D K & Yadav R R, *Open Acoust J*, 2 (2009) 61.

21 Hill R, *Proc Phys Soc A*, 65 (1952) 349.

22 Turkdal N, Deligoz E, Ozisik H, Ozisik H B, *Phase Trans*, 90 (2017) 598.

23 Weck P F, Kim E, Tikare V & Mitchell J A, *Dalton Trans*, 44 (2015)18769.

24 Morelli Donald T, Slack Glen A,Goela J, 18th Edn (Springer Publisher, 2006) 37.

25 Fine M E, Brown L D & Marcus H L, *Scripta Metallurg*, 18 (1984) 951.

26 Wang B B & Zhao Y P, IUTAM *Symposium on Surface Effects in the Mechanics of Nanomaterials and Heterostructures*, (2013) 31.

27 Rai S, Chaurasiya N & Yadawa P K, *Phys Chem Solid State*, 22 (2021) 687.

28 Liu X K, Zhou W, Liu X & Peng S M, *RSC Adv*, 5 (2015)59648.

29 Ivanovskii A L, *Int J Refract Met Hard Mater*, 36 (2013) 179.

30 Guechi A, Merabet A, Chegaar M, Bouhemadou A & Guechi N, *J Alloys Compd,* 623 (2015) 219.

31 Ranganathan S I & Ostoja-Starzewski M, *Phys Rev Lett*, 101 (2008) 55504.

32 Panda K B & Ravi Chandran K S, *Comput Mater Sci,* 35 (2006) 134.

33 Singh S P, Singh G, Verma A K, Yadawa P K & Yadav R R, *Pramana-J Phys*, 93 (2019) 83.

34 Jaiswal A K, Yadawa P K & Yadav R R, *Ultrasonics*, 89 (2018) 22.